

EFFECTS OF BIOCHAR ON SOIL WATER DYNAMICS

By

Erica Bempong

A Professional Paper Submitted in Partial Fulfilment

of the Requirements for the Degree

MASTER OF SCIENCE

Major Subject: Engineering

West Texas A& M University

Canyon, Texas

May 2026

## ABSTRACT

Biochar has been widely studied for its use as a soil supplement to improve soil water properties. Previous works indicate that the impacts of biochar are most significant in coarse-textured soils, but its impact on fine-textured soils is less often discussed. We investigated the prospects of cotton gin waste and beef cattle manure biochars in a laboratory setting, using varying particle sizes, (75-150  $\mu\text{m}$ , 150-425  $\mu\text{m}$  and 425-850  $\mu\text{m}$ ) and application rates (5, 10, 15 %) in silt clay loam collected from the cotton fields at the USDA-ARS Conservation and Production Research, Bushland, TX. Soil water characteristic curves (SWCC) were determined using the pressure plate extractor. The field capacity also referred to as water holding capacity (WHC), permanent wilting point (PWP) and plant available water (PAW) were obtained from this measurement. Saturated hydraulic conductivity ( $K_{sat}$ ) was measured using Humboldt permeameter with biochar sieved under 2 mm and the infiltration rates were calculated using Horton's equation.

The study evaluated the effects of cotton gin waste and beef cattle manure biochar on water holding capacity ( $WHC$ ), hydraulic conductivity ( $K_{sat}$ ) and infiltration rates ( $i$ ). Our results indicate that biochar enhanced WHC by 11.76% average in CGW amended soils and 47.05% average in BCM amended soils. The magnitude of change was strongly dependent on the feedstock and particle size. The results showed BCM biochar enhanced WHC more effectively than CGW, likely due to greater mesopore development. In contrast, CGW biochar increased macroporosity, significantly enhancing  $K_{sat}$  and infiltration rates. Across all particle sizes, the highest WHC were observed at 75-150  $\mu\text{m}$

particle size range across all feedstock. While all particle size ranges increased WHC substantially, they were independent of application rate. Also, air entry values ( $1/\alpha$ ) derived from SWCC showed an inverse relationship with WHC ( $R^2 = 0.2$ ), indicating a strong influence of pore size distribution on hydraulic behavior.

The findings demonstrate that biochar effects on soil water dynamics in silt clay loam (34% clay, 20% sand and 44% silt) are highly dependent on the feedstock material and particle size distribution, with minimum application rates interactions. Improvements in water holding capacity can be achieved at low rates (5%) whereas increasing rate of biochar rates leads to increase in ***K<sub>sat</sub>*** and infiltration rate

## **ACKNOWLEDGMENTS**

My thesis would not have been completed without my mentors and loved ones, and I express my deepest gratitude to those that helped me mentally on this journey.

I would like to express her sincere gratitude to Dr. Nathan Howell for taking a leap of faith in me in 2024 and entrusting me with this project. Thank you for your kindness, friendship and counsel.

A special thank you to all my committee members: Dr. Carolina Brandani, Dr. Pam Lockwood, Dr. Craig Bednarz for their dedication to shaping my thinking through their wonderful technical support and guidance.

I am grateful to West Texas A&M University, College of Engineering for giving me the opportunity to study and grow my academic aptitude.

Approved:

---

Chairman, Thesis Committee                      Date

---

Member, Thesis Committee                      Date

---

Member, Thesis Committee                      Date

---

Member, Thesis Committee                      Date

---

Associate Dean, College of Engineering                      Date

---

Dean, College of Engineering                      Date

---

Dean, Graduate School                      Date

## TABLE OF CONTENT

Abstract.....	ii
1. Introduction.....	1
2. Materials and Methods.....	5
2.1 Soil and biochar properties.....	5
2.2 Experimental treatments.....	6
2.2.1 Water holding capacity .....	6
2.2.2 Saturated hydraulic conductivity and Infiltration .....	8
2.2.3 Infiltration .....	8
2.2.4 Soil water characteristic curves .....	9
2.3 Statistical analysis .....	10
3. Results.....	1
4. Discussion.....	21
5. Conclusion .....	29
6. References.....	32

## List of figures

<b>Figure 1</b> Elemental analysis of biochar particle size range. Red line indicates separation between CGW and BCM biochar .....	3
<b>Figure 2</b> SEM images of particle size fractions. Top images show details of cotton gin waste biochar. Bottom images show details of beef cattle manure biochar .....	5
<b>Figure 3</b> Surface structure of soil–biochar mixtures as influenced by particle size and application rate. Top row: 75–150 $\mu\text{m}$ biochar at 5% (left) and 15% (right); bottom row: 425–850 $\mu\text{m}$ biochar at 5% (left) and 15% (right).....	6
<b>Figure 4</b> Changes in Soil Bulk Density Following Biochar Amendment at Different Application Rates and Particle Sizes .....	7
<b>Figure 5</b> Total soil volume change in soil bulk density across all particle size fractions and application rates. ....	8
<b>Figure 6</b> Effective porosity calculated across particle size fractions and application rates for both CGW and BCM biochar.....	9
<b>Figure 7</b> BET surface area, micropore surface area and mesopore surface area of biochar particle size fraction.....	10
<b>Figure 8</b> Infiltration rates of soil and soil-biochar treatments with 5%, 10% and 15% application rates .....	15
<b>Figure 9</b> Soil water characteristics curves for silt clay loam with CGW and BCM biochar (addition rate 5, 10 and 15%) across particle size fractions. The lines represent the fitted van Genuchten model .....	17
<b>Figure 10</b> Scatter plot diagram to compare average WHC across all particle size fractions to its mesopore area .....	23

## List of tables

<b>Table 1</b> Empirical values of the air entry values (kPa) for different soil texture classes.	10
<b>Table 2</b> Physical and chemical properties of soil and biochar material .....	2
<b>Table 3</b> Physicochemical characterization of the particle size fraction of the different feedstock .....	2
<b>Table 4</b> Volumetric water contents at PAW, FC and PWP determined from pressure plates. This table is for n = 5 measurements and the values are mean ± standard deviation .....	12
<b>Table 5</b> Hydraulic conductivity measurements for soil + biochar treatments across the three application rates .....	14
<b>Table 6</b> van Genuchten $\alpha$ and n values derived from different treatments using R software (* = inconclusive) .....	18
<b>Table 7</b> Three-way analysis of variance (ANOVA) for water holding capacity and bulk density as affected by feedstock type, application rate, and particle size, including all two-way and three-way interactions. Significance codes: '***' p < 0.001, '*' p < 0.05, '.' p < 0.1, 'ns' not significant.....	21

## **Nomenclature**

Plant available water (PAW): The amount of soil water that can be extracted by plants. Formally defined as the difference between field capacity and permanent wilting point

Field capacity (FC): The amount of water content held in soil after excess water has drained freely under gravity

Permanent Wilting point (PWP): Minimum amount of water in the soil plants require not to wilt

Water holding capacity (WHC): The amount of water that a given soil can hold for crop use. Also considered as FC

Water content: It is the measurement of the amount of water in the soil and defined as the water lost from soil upon drying to a constant mass at 105<sup>0</sup>C

Gravimetric water content (GWC): Related to mass of water per unit mass of dry soil. Expressed as g/g

Volumetric water content (VWC): Related to volume of water per volume of soil. Also equal to GWC times the soil's bulk density. Expressed as a percentage or cm<sup>3</sup>/cm<sup>3</sup>

Pyrolysis: Heating organic materials at high temperatures in the absence of oxygen

Particle size distribution: Description of relative amounts of particle of different sizes within a sample.

Porosity: The fraction of a material's bulk volume that is void space. Describes how much empty space exist. refers to the voids between sample particles which hold air and water

Pore size: A geometric measure of individual voids in a material's pores

Transient property: A characteristic of a material that changes over time before settling in a new condition

Matric potential: Defined as the portion of water potential that can be attributed to the attraction of the soil matrix for water.

Suction: Occurs when there is a difference in pressure, creating a vacuum and surrounding higher-pressure fluid rushes in to equalize

Air entry value (AEV): Minimum suction value required for entry of air into soil voids

## Effects of biochar on silt clay soil water dynamics

### AUTHORS

Erica Bempong<sup>a</sup>, Nathan Howell<sup>a\*</sup>, Lockwood Pamela<sup>a</sup>, Catherine Brandani<sup>d</sup>, Craig Bednarz<sup>de</sup>

<sup>a</sup>College of Engineering, West Texas A&M University, 2501 4<sup>th</sup> Ave, Canyon, TX, USA

<sup>b</sup>USDA Agricultural Research Service, Bushland, TX, USA

<sup>c</sup>Paul Engler College of Agriculture and Natural Science, West Texas A&M University

<sup>d</sup>Texas A&M AgriLife High Plains Research, Canyon, TX. Department of Soil and Crop Sciences, Texas A&M University, College Station, TX.

\*Corresponding author, [nhowell@wtamu.edu](mailto:nhowell@wtamu.edu)

### Highlights

- Hydraulic responses of silt clay loam after biochar addition were assessed.
- Biochar increased water holding capacity, improved hydraulic conductivity and infiltration, dependent on the feedstock type.
- Particle size fractions changed bulk density and total porosity of the soil matrix
- A 5% biochar application rate was sufficient to observe meaningful improvements in WHC/PAW

## 1. INTRODUCTION

Biochar, a carbon-rich material produced from the thermal degradation of biomass has become a promising solution for waste valorization and addressing pressing environmental challenges, including water pollution and soil degradation. Due to the low value of materials made from biochar, it fits into the waste-production transition and nowhere is it more valuable than in the developing world agriculture[1]. One of the benefits of biochar to the environment is the potential to improve water quantity such as water retention, plant available water, porosity, and permeability, while potentially driving the microbial community to positively affect the soils' environment, aeration and water percolation[2, 3]. Biochar is highly porous, and materials with high porosity have the ability to hold more matter (air, water and nutrients). In the Texas Panhandle region, beef and dairy cattle markets 6 million fed cattle annually in the Cattle feeding country (New Mexico, Texas and Oklahoma), and the amount of manure harvested shows 2.1 million dry metric tons of manure on a dry matter basis annually[4]. Additionally, cotton gin waste in Texas alone was approximately 8 million dry metric tons at the end of 2024[5] These abundant waste streams present a valuable opportunity for resource recovery, and conversion of these biomass materials to biochar could result in 1.05 and 3.2 million tons of biochar annually based on typical biochar yields of 50% and 32% for cotton gin waste and manure respectively. By processing these materials through conversion pathways, it is possible to reduce environmental burdens associated with waste disposal. It's also been reported that

biochar made from wood and straw based materials have the highest surface area and manure biochar has the highest N and P[6, 7]. These variations and structures can significantly affect soil physical and hydraulic properties.

Soil-water dynamics are crucial for agricultural productivity and water resource management, especially limited water environments such as the semi-arid environments of the Texas High Plains. Biochar has gained quite the attention over the years as a soil conditioner. The influence of biochar on soil health does not solely depend on the specific characteristics, but also on the quality and quantity of the biochar[8]. Produced through pyrolysis, it has the potential to alter soil structure when incorporated. Review papers by Edeh et al. and Adhikari et al. described biochar's effect on soil hydraulics as directly tied to the physical quality of biochar and thus, understanding the roles these qualities play will give a broader design selection criterion for biochar engineering specified for soil types and applications [9, 10]. Since biochar quality depends on the type of feedstock and pyrolysis conditions (e.g. temperature and time), its proficiency to change soil water quality and quantity depends on the combination of the biochar and soil properties[11-13]. The benefits of biochar amendment application in soil are more pronounced in a coarse-textured soil than a fine-textured soil, and thus clay-rich soils are less responsive than sandy soil[14]. Biochar is predicted to cause slow drainage in sandy soils and rapid drain in clay rich soils[15]. And so, the effect of biochar is dependent on the type of soil for hydraulic conductivity. Barnes et al. recorded a 328 % hydraulic conductivity increment in clay rich soil and one of the factors is that biochar alters the soil pore size distribution[16].

Commonly, biochar enhances soil water by altering the pore structure, decreasing bulk density and increasing total porosity and aggregation. The particle size fraction of biochar

is anticipated to have a key role in controlling water movement and storage [17, 18]. For example, soil hydraulic conductivity increased with decreasing particle size except for  $<0.063$  mm biochar-size in sandy loam and loamy sand soils whereas Liu et al reported a reduction in soil retention with the use of fine biochar ( $< 0.25$ mm) in sandy soil [18, 19]. Bulk densities in soils reported after biochar was applied at different rates shows a decline with coarser biochar particles than finer biochar particles [17, 20, 21]. This is because finer biochar particles tend to fill existing soil pore spaces, contributing less to the overall increase in bulk volume, whereas coarser biochar particles introduce and maintain larger inter-particle voids, resulting in a greater reduction in bulk density. The decrease in bulk density has been widely reported and found to increase porosity and improve overall soil aggregation [22, 23]. Porosity has been reported to play a role in soil water quantity: as larger, well-connected pores enhance infiltration and conductivity, smaller pores increase water retention [24]. Biochar particle size may influence the creation of new pores in the soil medium, increasing porosity within biochar particles (intraporosity) and between biochar and soil particles (interporosity), which controls water movement and has an impact in water storage [25, 26]. The addition of biochar fragments with different sizes will change the interporous characteristics and this affects water storage and movement [19]. Pore size distribution describing the size of pores are grouped into micropores ( $>2$ nm), mesopores (2-50 nm) and macropores ( $>50$  nm) and are known to contribute to soil's porosity. Micropores and mesopores are typically intrapore features and are suggested by Rasa et al., Pituello et al. and Wang H et al [25, 27, 28] to improve water retention and movement. Macropores can be both interpore and intrapore, but are especially relevant as interpore spaces when biochar is mixed into soil

Soil water is assessed through a range of hydraulic properties and in this study, we evaluate biochar-soil-water interactions via water holding capacity, hydraulic conductivity and infiltration rate. Water holding capacity (WHC) described as how much water is held under gravity, is synonymous to field capacity water content measured at -33kPa matric potential. Soil water characteristic curve (SWCC) is a visual plot of the volumetric water content versus the water potential and is greatly influenced by soil texture, particle size and pore structure[29-31]. These relationships are identified using the van-Genuchten model, and the shape parameters are assumed to change with biochar addition. The takeaway from this model is the air entry value (AEV) which is described as the tension where air enters, and water begins to drain, an indicative property of the soil pore structure and water infiltration characteristics. Few studies including Yang et al reported an air entry value of clay to be larger than sand[32].

We chose feedstocks varying with different chemical compositions to test the influence on biochar hydrologic properties in silt clay loam soil. We hypothesize that: (1) Biochar can hold more water and improve water retention in fine-grained soils (34% clay, 20% sand and 44% silt); (2) Biochar effects can largely influenced by application rates and particle size; (3) Maximum effects can be seen at lower dosage. These hypotheses were tested in lab scales. We constrained a group of properties (bulk density, surface chemistry and porosity) of the feedstocks selected and particle size distribution to provide valuable insights to end users who are considering biochar as a boost for a particular agroecosystem.

## **2. MATERIALS AND METHODS**

### **2.1 Soil and biochar properties**

Silt clay loam soil samples were collected from the conventional dryland cotton plot fields located at the ARS USDA Conservation and Production Research in Bushland, TX. The soil evaluated in this study is a representative of agricultural lands in the Texas Southern High Plains region. The biochars were made from cotton gin waste and beef cattle manure. The feedstock was ground and dried at 105°C for 24 hrs and subsequently pyrolyzed in a muffle furnace at 400°C for 1 hr. Biochars made at medium temperatures (400 °C -550 °C) increases micropores, mesopores and macropores in relevant biochar while preserving essential physical and functional groups that are all crucial for soil water improvement. The pH and EC measurements were conducted using a 1:5 mass ratio (sample: deionized water). Surface area (Brunauer-Emmett-Teller method) and pore structure were characterized by nitrogen (N<sub>2</sub>) physisorption at 77 K using a Micromeritics 3Flex surface characterization analyzer. Surface morphology was analyzed with Scanning Electron Microscope (Jeol Benchtop SEM). Both biochars were separated into different size fractions based on the d<sub>50</sub> of the soil (300 μm). Following fractionation into discrete particle size classes (75-150 μm, 150-425 μm, 425-850 μm) each biochar fraction was characterized for total organic carbon (TOC), elemental composition, and surface area. Pore size distribution was subsequently determined from surface area analysis, employing the t-plot method to quantify micropore area and the BJH adsorption–Halsey thickness curve to characterize mesopore distribution.

Soil amendments were prepared by mixing the silt clay soil with biochar at three weight-based ratios. The terms CGW5, CGW10 and CGW15 are used to identify the 5%, 10%, and 15% cotton gin waste biochar levels, while BCM5, BCM10 and BCM15 are used to identify beef cattle manure biochar levels. There is only one biochar formulation for each feedstock (CGW or BCM). We used no nomenclature to differentiate pyrolysis or post-pyrolysis conditions. The bulk densities were determined using the dry mass of samples and total sample volume and total porosity (volume fraction of intrapores and interpores) and effective porosity (interpores) were calculated using Equation 1

$$1 - \frac{\left(\frac{M_s}{p_{ss}} - \frac{M_b}{p_{sb}}\right)}{V} \quad \text{Equation 1}$$

where  $M_s$  and  $M_b$  (g) are mass of silt clay loam soil and biochar, respectively.  $p_{ss}$  and  $p_{sb}$  are the particle densities ( $\text{g}/\text{cm}^3$ ) of both silt clay loam soil and biochar, respectively.

The particle densities for each feedstock were obtained from published literature as direct measurement was not conducted. A value of  $1.36 \text{ g}/\text{cm}^3$  for mesquite wood biochar pyrolyzed at  $400^\circ\text{C}$  from Brewer et al. was adopted for the CGW biochar as they are both lignocellulose feedstocks with comparable pyrolysis conditions[33]. For BCM biochar, a particle density of  $1.66 \text{ g}/\text{cm}^3$  was reported by Tsai et al. for dairy cattle manure, given that they both are manure-derived feedstocks with comparable mineralogical characteristics[34].

## 2.2 Experimental treatments

### 2.2.1 Water holding capacity

The biochars were sieved into three size-fractions: 75-150  $\mu\text{m}$ , 150-425  $\mu\text{m}$ , and 425-850  $\mu\text{m}$  which are designed by the  $d_{50}$  of the soil (300  $\mu\text{m}$ ). Sieving was done using an

automated sieve shaker designed by the Senior Design Group (*The Gentle Sieve Shaker*, West Texas A&M University, 2018), for 15 min with sieve sizes 75  $\mu\text{m}$  (US Sieve No.200), 150  $\mu\text{m}$  (US Sieve No.100), 425  $\mu\text{m}$  (US Sieve No.40) and 850  $\mu\text{m}$  (US Sieve No. 20).

The biochars were mixed with soil samples at three application rates (5, 10 and 15%). The soil water content and soil + biochar mixtures at pressures 0.33, 5, 7, 10 and 15 bars were measured using the 1500F2 Pressure Plate Extractor and 1600 Pressure Plate Extractor from Soil Moisture Instrument Company. The pressure plate is an approach to measure suction directly and employs the use of saturated ceramic plate to separate pore air pressure and pore water pressure on the samples, and then the suction is controlled by applying pore air pressure. The procedure follows the ASTM C1699-09. Samples were thoroughly mixed, placed in rings on ceramic plates and saturated for at least 24 hrs. The wet mass samples after the equilibration period were measured and oven oven-dried to obtain the mass of the dry samples.

The data collected was used to calculate gravimetric and volumetric water content at the different suctions. All measurements had 5 replicates. The gravimetric water content (GWC) was calculated using Equation 2

$$GWC = \frac{W_f - D}{D} \quad \text{Equation 2}$$

where  $W_f$  is the final weight of the sample (g) and  $D$  is the dry weight of the sample (g). Finally, we converted the volumetric water content (VWC:  $\text{cm}^3/\text{cm}^3$ ) to GWC(g/g) using bulk density ( $\text{g}/\text{cm}^3$ ) as provided in Equation 3,

$$VWC(cm^3/cm^3) = GWC * \rho_b \quad \text{Equation 3}$$

Depending on the suction, the measuring time varied. For instance, a complete extraction of water at 0.33 bar takes around 4 days, while at 15 bars, it takes about 32 days. When water outflow ceases or declines to a few drops per day, we state that the soil is in equilibrium at each pressure level. The testing was accelerated by the inclusion of two pressure chambers and the capacity to stack up to four ceramic plates. From the data collected, we calculated the water content at commonly accepted values for field capacity (FC) and permanent wilting point (PWP) (0.33 and 15 bars, respectively), which were used to calculate the plant available water (PAW; Equation 4)

$$PAW = FC - PWP. \quad \text{Equation 4}$$

### 2.2.2 Saturated hydraulic conductivity and Infiltration

The soil and biochars samples were sieved to  $\geq 2mm$  and biochar was applied at 5, 10 and 15%. After saturation, the samples were set up in permeameter and saturated  $\geq 48$  hrs and measurements were recorded. Saturated hydraulic conductivity of each sample was measured in triplicate with HUMBOLDT permeameter. The instrument employs both failing head and the constant head permeability test but for this test only the failing head was employed, which is typically used for fine-grained soils. The saturated hydraulic conductivity was determined using Variable head Permeability Formula:

$$K = \frac{2.303V_wL}{(h_1-h_2)tA} \log \frac{h_1}{h_2} \quad \text{Equation 5}$$

where  $t$  = time recorded (min),  $V_w$  = volume of water drained (ml),  $L$  = length of the permeameter(cm),  $A$  = area of the permeameter ( $\text{cm}^3$ ) and  $h_1$  and  $h_2$  (cm) are the initial and final height of water in the column.

### 2.2.3 Infiltration

Infiltration was analyzed using the Robert E. Horton model (Equation 6) which presents the empirical description of infiltration behavior rather than a mechanistic hydraulic model. It describes the exponential decline in infiltration as soil becomes progressively wet.

$$f(t) = f_c + (f_0 - f_c) e^{-kt} \quad \text{Equation 6}$$

where:  $f(t)$  = infiltration rate at time  $t$  [ $\text{cm h}^{-1}$ ] at infiltration rate at time  $t$ ;  $f_c$  = final (minimum) infiltration rate, representing the saturated hydraulic conductivity of the soil [ $\text{cm h}^{-1}$ ];  $f_0$  = initial (maximum) infiltration rate at the start of the event ( $t = 0$ ) [ $\text{mm h}^{-1}$ ];  $k$  = Horton's decay constant, governing the rate at which infiltration capacity decreases over time [ $\text{h}^{-1}$ ]

The steady state infiltration rate obtained from the Horton model was interpreted as an indicator of the soil's equilibrium infiltration capacity which is closely related to the saturated hydraulic conductivity.

### 2.2.4 Soil water characteristic curves

Soil water characteristic curves, also known as water retention curves, were determined using the pressure points (matric potential) and VWC from the water holding capacity measurements. The van Genuchten model (van Genuchten,1980) was used to analyze the soil water retention curves (Equation 7).

$$\theta = \theta_r + (\theta_s - \theta_r)[1 + (\alpha h)^n]^{-m} \quad \text{Equation 7}$$

where  $\theta_r$  is residual water content ( $\text{cm}^3/\text{cm}^3$ ),  $\theta_s$  is saturated water content ( $\text{cm}^3/\text{cm}^3$ ),  $\alpha$  is the inverse of the air entry pressure (kPa),  $n$  and  $m$  are empirical shape parameters and  $h$  is the tension potential (kPa). The fitting parameters were extracted using the R software (soil physics Comprehensive R Archive Network (CRAN)). The air entry level which is equal to the inverse of  $\alpha$  is important to determine the permeability of the soil. Typical air-entry values for soils with different textures were provided by Rawls et al.[35]

**Table 1** Empirical values of the air entry values (kPa) for different soil texture classes

Soil texture	Clay	Silty clay	Sandy clay	Clay loam	Silty clay loam	Sandy clay loam	Loam	Silt loam	Sandy loam	Silt	Loamy sand	Sand
Value	37.30	34.19	29.17	25.89	32.56	28.08	11.15	20.76	14.66	20.00	8.69	7.26

The air entry value for the silt clay loam soil used in this study was 32.56 kPa which was adopted as a representative reference for comparative evaluation

### 2.3 Statistical analysis

Bulk density and field capacity were analyzed using the R software. Two separate ANOVA multi-way ANOVA were conducted: (1) test the effects of biochar application rate, particle size distribution and their interactions with CGW biochar(fixed) and (2) test the effects of biochar application rate, particle size distribution and their interactions with BCM. Each ANOVA were conducted separately biochar and this approach allowed for full factorial analysis within each feedstock type while reflecting the independence of the two feedstock experiments.

### 3. RESULTS

#### 3.1 Soil and Biochar Characterization

The physicochemical characterization of the clay loam soil and the biochars made at 400°C are displayed in Table 2. The native soil presented a slightly acidic pH of 6.7 and a low conductivity of 0.43 mS/cm, which defines it as an alkaline and non-saline soil texture according to NRCS, USDA[36]. Cotton gin waste (CGW) and beef cattle manure (BCM) biochars were strongly alkaline with CGW biochar having a pH of 11.1 and BCM biochar a pH of 10.5. Electrical conductivity recorded was higher in the biochars than the soil. CGW and BCM biochar showed an EC of 75 mS/cm and 12.2 mS/cm respectively.

Total organic carbon content differed substantially across the three media. Silt clay loam exhibited a low TOC of 1.12%, while CGW and BCM biochars reported higher values of 29.39% and 35.02%. This is consistent with pyrolytic conversion of organic feedstocks into carbon rich materials. Bulk density further distinguished the materials, with the biochars being lighter than the native soil. The bulk density depends on the material from which it is made from, and at 400°C, the bulk density varied with the same residence time. The finding showed a close value reported by Borhan et al that found the bulk density of BCM biochar to be 0.76g/cm<sup>3</sup> [37]. Total organic carbon will also be more compared to the original soil. Collectively, these data indicate the chemical and physical differences between soil and the biochars and when mixed together, they will be an alternate change with the magnitude of these changes governed by biochar type.

**Table 2** Physical and chemical properties of soil and biochar material

Property	Soil	CGW (bulk)	BCM (bulk)
pH	6.7	11.1	10.5
Electrical Conductivity (mS/cm)	0.43	7.5	12.2
Bulk density(g/cm <sup>3</sup> )	1.36	0.45	0.61
Total organic carbon (% weight)	1.12	29.39	35.02
BET surface area (m <sup>2</sup> /g)	-	4.88	4.30
d <sub>50</sub> (mm)	0.30	0.75	2.0

Characterization was also undertaken on the particle size fractions to show compositional differences and how these properties may directly influence soil behavior following amendments, and these are presented in Table 3. The TOC% recorded for individual CGW fractions were comparable to those of the unseparated bulk CGW, suggesting that fractionation did not result in appreciable organic carbon partitioning between size classes. The BET surface area (SA) exhibited a significant value of 11.42 m<sup>2</sup>/g for the 75-150 μm range, followed by 9.05 m<sup>2</sup>/g for the 425-850 μm range. The 150-425 μm range recorded the lowest SA at 2.75 m<sup>2</sup>/g.

**Table 3** Physicochemical characterization of the particle size fraction of the different feedstock

Property	CGW					BCM				
	Particle Size Fractions					Particle Size Fractions				
	<75 μm	75–150 μm	150–425 μm	425–850 μm	>850 μm	<75 μm	75–150 μm	150–425 μm	425–850 μm	>850 μm
Bulk density(g/cm <sup>3</sup> )	0.43	0.67	0.56	0.37	0.21	0.58	0.62	0.56	0.33	0.30
BET Surface area (m <sup>2</sup> /g)	4.50	13.35	2.61	6.88	2.26	9.83	9.25	4.66	4.37	2.89
Surface area (m <sup>2</sup> /g /C)	13.41	38.29	7.46	15.73	3.85	26.98	24.43	13.34	11.89	7.83
O/C ratio	0.21	0.20	0.20	0.19	0.15	0.16	0.18	0.16	0.17	0.16
H/C ratio	0.54	0.54	0.54	0.48	0.38	0.69	0.68	0.62	0.63	0.63

Surface area has been reported to be large in biochar[38]. For example, Haider reported a BET surface area of 50.2 m<sup>2</sup>/g for switchgrass-derived biochar, while Howell reported a considerably higher BET surface area of 490 m<sup>2</sup>/g for cottonseed biochar[39, 40]. In our analysis, surface area was smaller compared to these reports and also, the surface area of the bulk biochars differed from the particle size fractions. Surface area in CGW biochar recorded were high for 75-150 μm (13.35 m<sup>2</sup>/g) and 425-850 μm (6.88 m<sup>2</sup>/g), and a low SA for 150-425 μm (2.61 m<sup>2</sup>/g). You would expect SA to decrease as particle size increases. However, BCM followed the conventionally expected inverse relationship between particle size and surface area, as particle size increases, SA decreases from 9.25 - 4.37 m<sup>2</sup>/g.

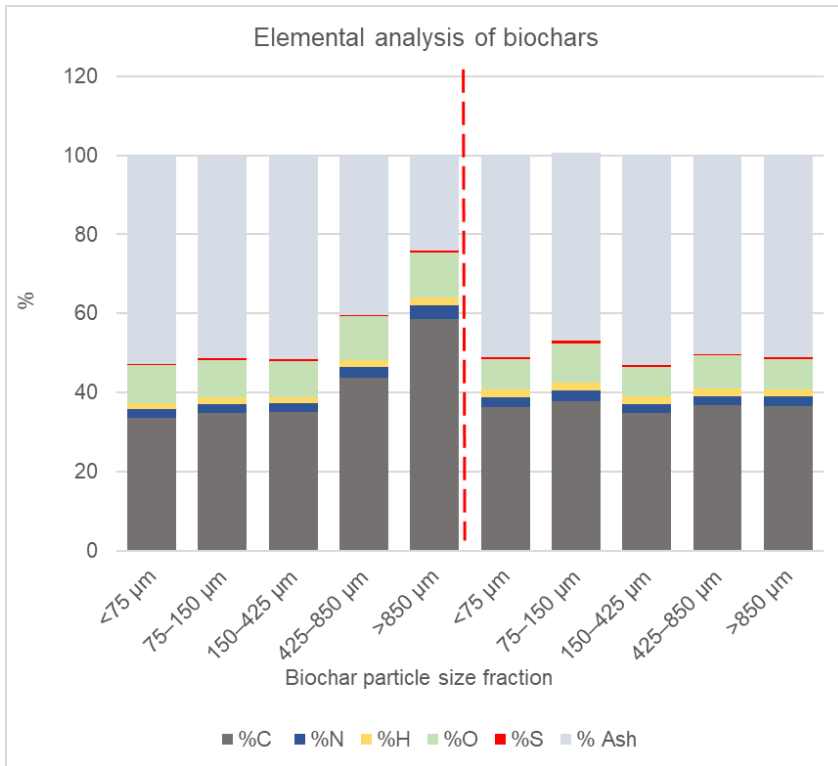


**Figure 1** Elemental analysis of biochar particle size range. Red line indicates separation between CGW and BCM biochar

The elemental ratios O/C and H/C were analyzed to detect functional groups and aromaticity of the biochars. The O/C ratios (0.15–0.21) suggest that biochars with higher oxygen content exhibit greater hydrophilicity, which enhances water retention through increased surface functional groups. Conversely, lower O/C ratios indicate a more hydrophobic character, reducing water adsorption. The H/C ratios (0.38–0.69) indicate varying degrees of aromaticity, where lower values correspond to more condensed structures that may promote microporosity and water retention at higher tensions. To buttress the H/C ratio result, an acid hydrolysis test was conducted with sulphuric acid ( $\text{H}_2\text{SO}_4$ ) to detect recalcitrant carbon and it showed that CGW carbon was more recalcitrant (close to the TOC%) while BCM reported a 16.12% recalcitrant carbon, making it a labile carbon material.

### **3.2 Morphology Analysis of Biochars**

Scanning electron microscope images (SEMs) are provided for CGW and BCM biochar in Figure 2. Both CGW and BCM biochar exhibited porous and irregular structures which are characterized by the feedstock type. There are a few subtle differences that can be pointed out here especially in surface texture. The 75-150  $\mu\text{m}$  CGW biochar shows high agglomeration and smaller particles compared to BCM within the same particle size fraction which appears to have more free gaps between larger particles.

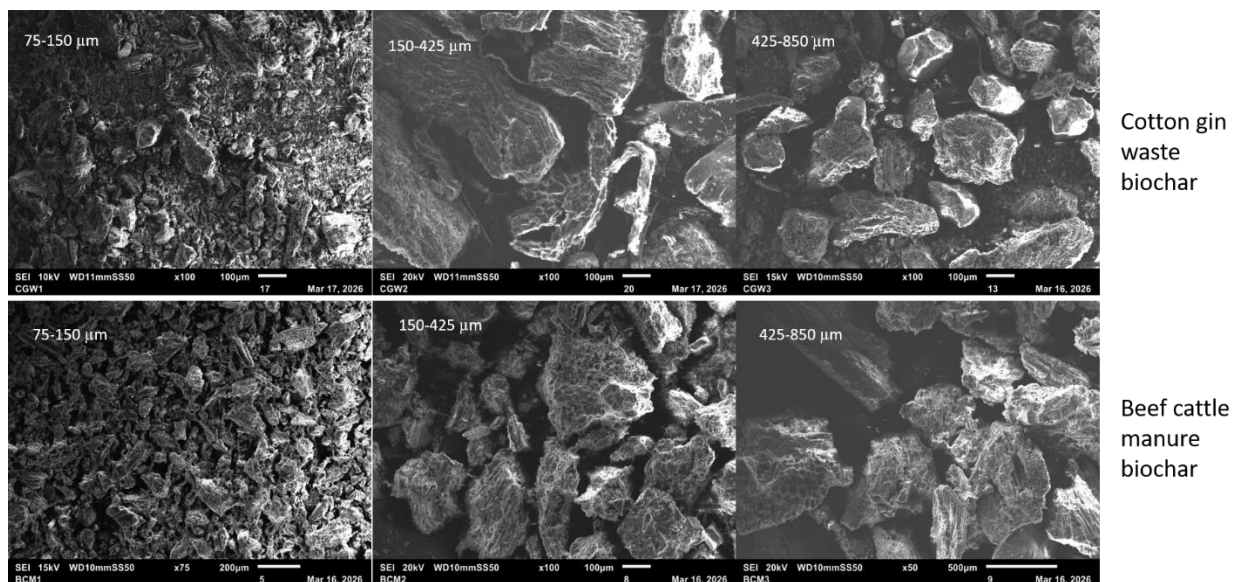


**Figure 2** SEM images of particle size fractions. Top images show details of cotton gin waste biochar. Bottom images show details of beef cattle manure biochar

Larger particles (150-850  $\mu\text{m}$ ) exhibited a more distinct angular and layered surface, showing visible rough, sharp surfaces. It was also observed that although the 75-150  $\mu\text{m}$  held the smallest sizes, the images of the larger particles contain smaller-sized particles which may be due to sieve transferring or the accommodating them in their pores. In Figure 3, the top two images show the addition of 75-150  $\mu\text{m}$  biochar at 5% and 15% application rate. Both treatments exhibited smooth and uniform surfaces with the 15% resulting in a darker, more uniformly coated appearance. The bottom two images show the biochar at 425-850  $\mu\text{m}$  sized particles, which is a coarser structure compared to the 75 -150  $\mu\text{m}$ . The particles are clearly distinguishable, forming a heterogenous and rough surface. The effect at 15% biochar application rate is amplified, due to the greater amount of biochar particles, with finer particle size appearing to be integrated more homogenously with the soil than the larger particle size, which appears to be looser.

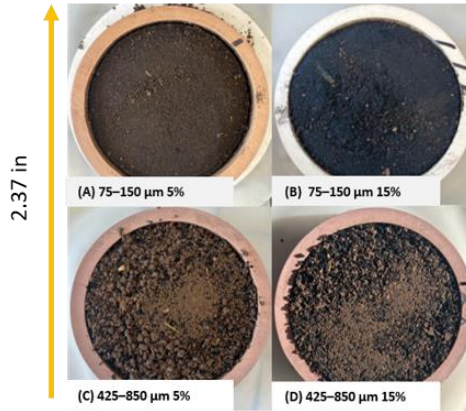


**Figure 3** Surface structure of soil–biochar mixtures as influenced by particle size and application rate. Top row: 75–150  $\mu\text{m}$  biochar at 5% (left) and 15% (right); bottom row: 425–850  $\mu\text{m}$  biochar at 5% (left) and 15% (right)

### 3.3 Effect of CGW and BCM biochar addition on soil bulk density and porosity

Biochar when added to a soil, changes the volume of soil. Significant changes in bulk densities between the biochar particle sizes at different application rates with silt clay loam soil are presented in Figure 3. Soil bulk density ( $\rho_{\text{bulk}}$ ) of both addition of CGW and BCM biochars decreased as the application rate increased and the particle size increased. The natural  $\rho_{\text{bulk}}$  of the silt clay loam was measured to be 1.36  $\text{g}/\text{cm}^3$  and from Table 2, the  $\rho_{\text{bulk}}$  obtained for CGW and BCM biochars were 0.45 and 0.61  $\text{g}/\text{cm}^3$  respectively. Soil amended with CGW biochar had a  $\rho_{\text{bulk}}$  ranging from 1.24 to 1.21  $\text{g}/\text{cm}^3$  at 5% as the particle size increased, while BCM biochar had a higher range from 1.28–1.32  $\text{g}/\text{cm}^3$ . The effect was more pronounced at 10% and 15% rates, with BCM biochar consistently resulting in a higher  $\rho_{\text{bulk}}$  than CGW biochar under equivalent treatments. Zhang et al. reported application of 2% rouge biochar with particle size  $<500 \mu\text{m}$  decreased the bulk density in clay soil by 4.3% [26]. For both biochars, the largest particle size fraction (425–850  $\mu\text{m}$ ) had the lowest  $\rho_{\text{bulk}}$  values at each application rate. Comparing with the control soil  $\rho_{\text{bulk}}$  (silt clay loam), all biochar amended treatments showed reduced bulk density values.

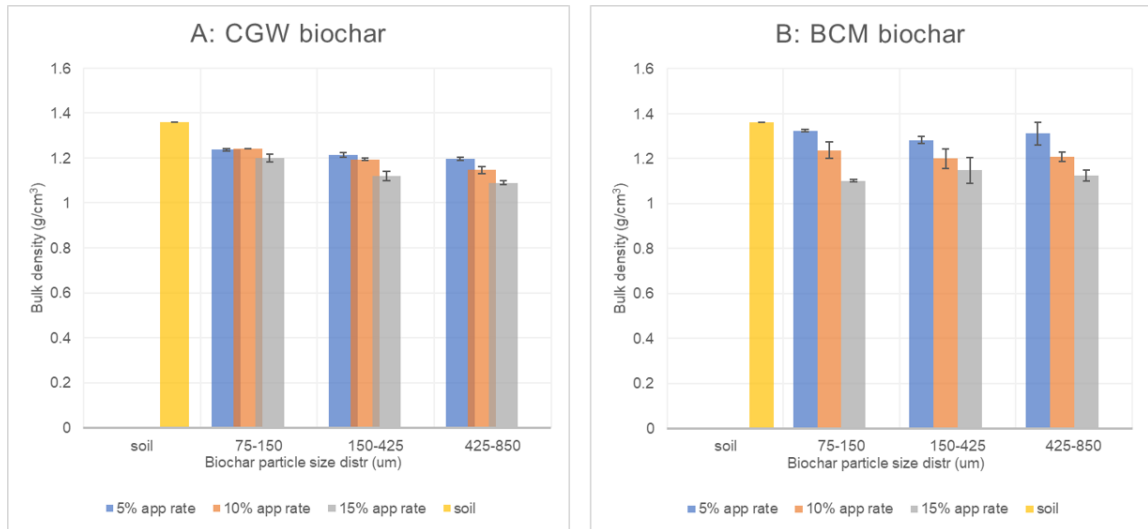


**Figure 4** Changes in Soil Bulk Density Following Biochar Amendment at Different Application Rates and Particle Sizes

The total volume,  $V_T$  in the soil changed as biochar was added as seen in Figure 4. The red line in the graph depicts the reference volume which is  $1 \text{ g/cm}^3$  in our case. For the 5% amendment rate, the total volume percent increase ranged from 5% to 15%; for the 10% rate, from 10% to 31%; and for the 15% rate, from 15% to 47%. The size fraction 425-850  $\mu\text{m}$  particle size fractions recorded the highest  $V_T$  across all feedstock and application rates. We run an RCBD (randomized complete block design) with the feedstock as the block and the p values were below 0.05 for both size and application rate. While the type of feedstock had an effect in the overall bulk density, the particle size and the app rate have a higher influence on the total volume of the soil.

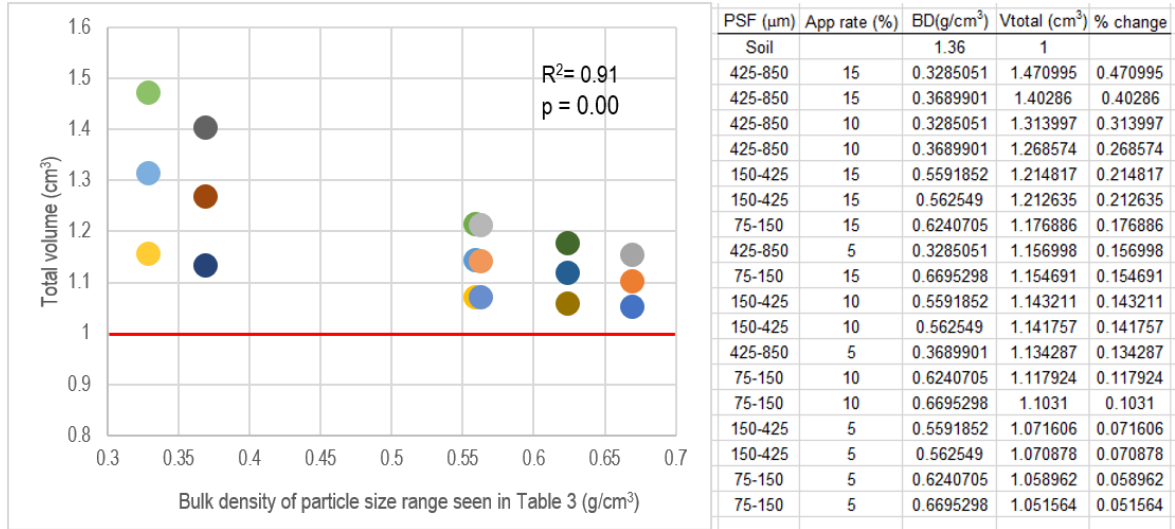


**Figure 5** Total soil volume change in soil bulk density across all particle size fractions and application rates.

Also, the weighted average  $\rho_b$  was calculated for each application rate. Each sample had a mass of 25g, which is equivalent to 0.33 mass fraction. For CGW 5 and BCM 5 treatments, the deviations from individual particle size  $\rho_{bulk}$  from the weighted average were within  $\pm 0.02 \text{ g/cm}^3$ . CGW 10 and BCM 10 recorded a deviation within a range of +0.05 to -0.05  $\text{g/cm}^3$ . CGW 15 showed a deviation within 0.06 to 0.05  $\text{g/cm}^3$  while within BCM 15  $\pm 0.02 \text{ g/cm}^3$  respectively. Since the weight fraction is constant across all treatments, the data strongly suggest that the bulk density is influenced by both the application rate and particle size fractions.

The total porosity ( $\phi_T$ ) of the soil (control) was 0.47, indicating the total soil pore volume. Addition of biochar at the three application rates increased by a 28% (approx. 0.60) across application rates for both feedstocks. No clear trend was observed with the application rate increasing.

The effective porosity ( $n_e$ ), which is the interparticle connected pores showed different changes across the particle size fractions and the application rates. Overall, biochar

amendment increased effective porosity above the control for majority of the treatments. CGW 10, CGW 15 and BCM 5 at 75-150  $\mu\text{m}$  particle size recorded lower values of  $n_e$ . These treatments recorded the higher bulk densities and may have had a direct effect on their  $n_e$  compared to the other treatments. An indication of a lower effective porosity shows there are more intrapores than interpores in these treatments compared to the others. To better understand the mechanism by which biochar porosity may affect soil water properties., it is necessary to evaluate the internal pore structure within biochar. While our study does not directly characterize inter and intra porosity, attributing primary WHC to the spaces between biochar particles will agree with Liu et al. [19], who reported that intrapores increases field capacity and plant available water overall.

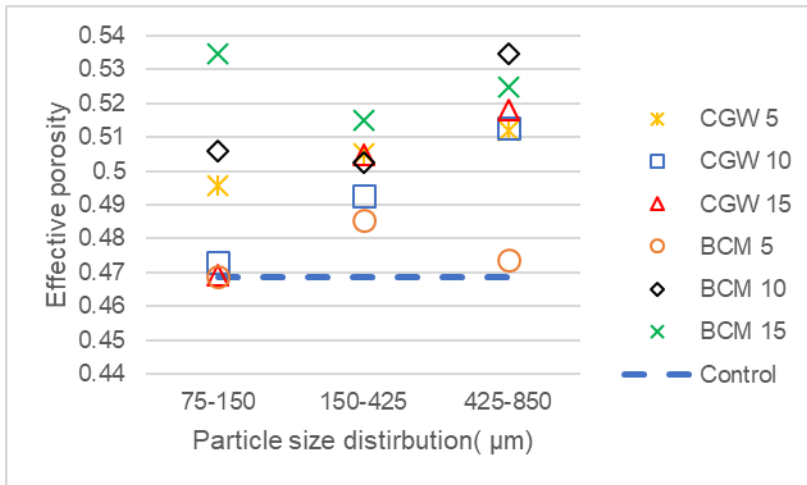


**Figure 6** Effective porosity calculated across particle size fractions and application rates for both CGW and BCM biochar

In both feedstocks, the 75–150  $\mu\text{m}$  fraction exhibited the highest pore surface areas, with CGW recording the greatest BET and mesopore surface areas of approximately 13.35 and 11.86  $\text{cm}^2/\text{g}$  respectively, suggesting that finer particles possess a greater total and mesopore-specific surface area. Surface area declined markedly with increasing particle

size in CGW, with the 150–425  $\mu\text{m}$  fraction recording the lowest values before a partial recovery was observed in the 425–850  $\mu\text{m}$  fraction in. BCM followed a similar trend, though with consistently lower BET and mesopore surface areas across all fractions compared to CGW. Micropore surface areas were comparatively low across both feedstocks and all size fractions. Negative micropore values were recorded for both CGW and BCM biochar in the 150–425  $\mu\text{m}$  fraction which indicates the absence of measurable micropores within the particle size range. Our findings suggest that micropores predominate more in particles below 75  $\mu\text{m}$ .

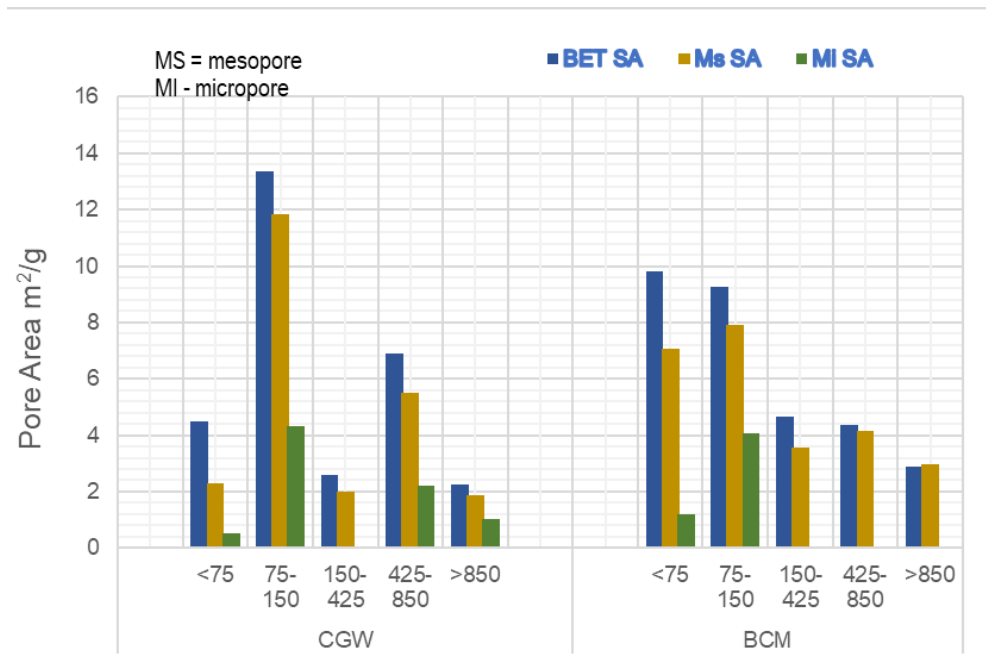


**Figure 7** BET surface area, micropore surface area and mesopore surface area of biochar particle size fraction

### 3.4 Effects of CGW and BCM biochar on water holding capacity and plant available water

Water holding capacity, also known as field capacity water content refers to the ability of soil to retain water after excess drainage. Plant available water is the portion that can be

taken up by plant roots. Together, these two properties reflect how well a soil can store and supply water to plants. The plant available water ( $\theta_{paw}$ ) were determined using the measurements of volumetric water content,  $\theta$  at field capacity (-0.33 bar or -33kPa) and permanent wilting point (-15 bar or -1500 kPa). Data on plant available water, field capacity and permanent wilting point are listed in Table 4. Field capacity water content ( $\theta_{fc}$ ) or water holding capacity (WHC) for unamended soil was  $0.34 \text{ cm}^3/\text{cm}^3$ . With CGW amendment, field capacity showed a general trend of increasing field capacity with increasing application rate, though the response was inconsistent across particle size fractions. At CGW5,  $\theta_{paw}$  increased by 8.8%, 5.9%, and 14.7% in 75-150  $\mu\text{m}$ , 150-425  $\mu\text{m}$  and 425-850  $\mu\text{m}$  respectively across all feedstock. At 10%, 75-150  $\mu\text{m}$  gave a higher  $\theta_{paw}$  but the coarser fractions dropped below the control (i.e. -5.9% and -2.9%). At 15% application rate, CGW remained moderate, with similarly mixed positive and negative deviations from the control across particle sizes. The data shows CGW biochar particle size and application rates had a moderate to minimal effect on field capacity content except for the smaller particle size 75-150  $\mu\text{m}$  which consistently boosted field capacity water contents for all application rates.

Field capacity ( $\theta_{fc}$ ) values for BCM biochar amended soils were higher than both the CGW amended soils and the unamended soil. At the 5% application rate, field capacity increased by 32.4%, 32.4%, and 8.8% across the 75-150, 150-425, and 425-850  $\mu\text{m}$  fractions, respectively. At 10%, the finest fraction (75-150  $\mu\text{m}$ ) yielded the highest observed field capacity across the entire dataset ( $0.49 \text{ cm}^3/\text{cm}^3$ ), representing a 44.1% increase over the control, while the 150-425  $\mu\text{m}$  and 425-850  $\mu\text{m}$  fractions increased by

29.4% and 17.6%, respectively. At the 15% application rate, field capacity remained elevated across all fractions at 35.3%, 26.5%, and 11.8% above the control.

Across all BCM treatments, the finest particle size fraction (75-150  $\mu\text{m}$ ) consistently produced the highest field capacity values, mirroring the trend observed with CGW biochar. However, unlike CGW, BCM biochar demonstrated a more uniform and robust improvement across all particle sizes and application rates, BCM may have some physical or chemical properties that provide an advantage in increasing water retention.

**Table 4** Volumetric water contents at PAW, FC and PWP determined from pressure plates. This table is for  $n = 5$  measurements and the values are mean  $\pm$  standard deviation

	Treatments	App rate (%)	Particle size distribution ( $\mu\text{m}$ )	Volumetric Water Content ( $\theta$ )		
				Field Capacity	Permanent Wilting Point	Plant Available Water
<i>Mixtures</i>	Soil			$0.34 \pm 0.02$	$0.20 \pm 0.02$	$0.13 \pm 0.03$
	Soil + CGW biochar	5	75-150	$0.37 \pm 0.02$	$0.18 \pm 0.00$	$0.18 \pm 0.02$
		10	75-150	$0.40 \pm 0.02$	$0.18 \pm 0.02$	$0.22 \pm 0.03$
		15	75-150	$0.35 \pm 0.03$	$0.17 \pm 0.00$	$0.18 \pm 0.03$
		5	150-425	$0.36 \pm 0.01$	$0.19 \pm 0.01$	$0.17 \pm 0.01$
		10	150-425	$0.32 \pm 0.02$	$0.19 \pm 0.01$	$0.13 \pm 0.02$
		15	150-425	$0.33 \pm 0.02$	$0.19 \pm 0.00$	$0.14 \pm 0.02$
		5	425-850	$0.39 \pm 0.01$	$0.18 \pm 0.03$	$0.21 \pm 0.03$
		10	425-850	$0.33 \pm 0.03$	$0.18 \pm 0.00$	$0.15 \pm 0.03$
		15	425-850	$0.36 \pm 0.03$	$0.18 \pm 0.02$	$0.18 \pm 0.03$
	Soil + BCM biochar	5	75-150	$0.45 \pm 0.05$	$0.13 \pm 0.02$	$0.32 \pm 0.05$
		10	75-150	$0.49 \pm 0.05$	$0.14 \pm 0.00$	$0.34 \pm 0.05$
		15	75-150	$0.46 \pm 0.01$	$0.30 \pm 0.03$	$0.16 \pm 0.03$
		5	150-425	$0.45 \pm 0.01$	$0.14 \pm 0.01$	$0.31 \pm 0.01$
		10	150-425	$0.44 \pm 0.03$	$0.17 \pm 0.06$	$0.27 \pm 0.07$
		15	150-425	$0.43 \pm 0.01$	$0.13 \pm 0.01$	$0.31 \pm 0.01$
		5	425-850	$0.37 \pm 0.02$	$0.11 \pm 0.01$	$0.26 \pm 0.03$
		10	425-850	$0.40 \pm 0.03$	$0.20 \pm 0.01$	$0.21 \pm 0.03$
		15	425-850	$0.38 \pm 0.05$	$0.15 \pm 0.02$	$0.22 \pm 0.06$

Permanent wilting point  $\theta_{pwp}$  did not have any significant effect under CGW across all particle size fractions and application rates. However, a different trend is seen in BCM amendments. BCM 150-425  $\mu\text{m}$  significantly added a 50% increase at 15% app rate and

decreased at 5 and 10%. BCM across all particle size fractions had a negative effect on  $\theta_{pwp}$ . It decreased the water contents to as low as  $0.11 \text{ cm}^3/\text{cm}^3$ . Similar trend has been reported in literature, that biochar amendments increased field capacity whereas as permanent wilting point was not as much affected [3, 41]. But in our case, the type of feedstock determines the effect at permanent wilting point.

Plant available water ( $\theta_{paw}$ ) was strongly affected due to the significant effect at ( $\theta_{fc}$ ). Increasing application rate beyond 5% did not improve water availability and in some cases, reduced it, particularly for BCM. Across both feedstocks, increasing application rate did not consistently improve PAW retention, suggesting that feedstock type and particle size interact to influence water availability in ways that are not strictly dose-dependent.

### **3.5 Effect on hydraulic conductivity and infiltration**

Results from the saturated hydraulic conductivity measurements varied with both biochars and application rate. The control sampled produced a  $K_{sat}$  value of  $0.13 \text{ cm/hr}$ . When CGW biochar was added, there was a progressive increase in the  $K_{sat}$  as the application rate increased. At 5%, CGW and BCM biochar did not show any significant change. The most pronounced effect was seen when CGW biochar was applied at 10% and 15%. The substantial enhancement relative to the application rates suggests that a higher incorporation significantly improves soil permeability.

**Table 5** Hydraulic conductivity measurements for soil + biochar treatments across the three application rates

Treatment	'+ biochar	Hydraulic conductivity (cm/hr)
soil		0.13 ± 0.13
cotton gin waste	5	0.08 ± 0.10
	10	0.24 ± 0.22
	15	1.05 ± 0.78
beef cattle manure	5	0.10 ± 0.04
	10	0.60 ± 0.32
	15	0.17 ± 0.11

BCM at 10% surged up to a 0.60cm/hr but decreased at 15%.  $K_{sat}$  according to Rawls et al. [42] Green - Ampt references shows that our soil, silt clay loam has a  $K_{sat}$  of 0.10 cm/hr and Ajayi et al reported a  $K_{sat}$  of 0.22 cm/hr in silt clay loam with wood biochar [22]. The range seen here may likely be due to the location of the biochar in the soil column.

Infiltration rates  $f(t)$  exhibited characteristic exponential decline over time for all treatments across the CGW treatments, consistent with the Horton infiltration model. Initially, all soil showed a relatively high infiltration rates, followed by a rapid decrease within the 10-20 minutes and eventually approached a steady state rate which is equivalent to the  $K_{sat}$  values. After approximately 20 minutes, the CGW15 treatment exhibited the highest equilibrium rate, followed by CGW10 and CGW5, while the unamended soil remained significantly lower. Among all the treatments, CGW biochar demonstrated a notable higher initial infiltration rates compared to the control soil. CGW 15 showed the higher infiltration rate (0.21 cm/min) at the beginning, followed by CGW 10 (0.07 cm/min). CGW 5 did not have a much effect as it can be seen that the infiltration rate was similar to the control (0.03-0.04 cm/min).

BCM5, BCM10 and BCM15 initial infiltration rates started slow at 0.018, 0.02 and 0.025 cm<sup>3</sup>/min respectively and were lower than soil infiltration rate however, it kept a consistent steady state infiltration over time which were higher than CGW5, CGW10 and CGW15. The Horton model proposes that, over time, the infiltration rate will converge with the  $K_{sat}$ . BCM indicates that water penetrates the soil at a constant pace without variation, while CGW exhibits a significant initial surge in infiltration. This phenomenon may also be characterized in relation to the pore. CGW may possess a greater quantity of macropores to facilitate drainage; but, when it reaches sections with fewer macropores, water is retained more tightly, resulting in less water movement compared to previous conditions.

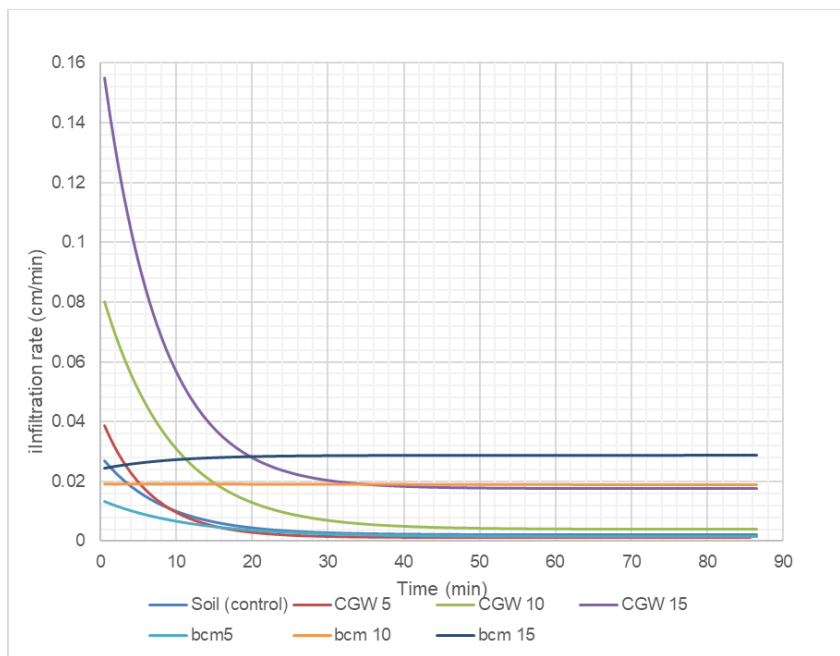


**Figure 8** Infiltration rates of soil and soil-biochar treatments with 5%, 10% and 15% application rates

### 3.6 Soil water characteristic curves (SWCCs)

For the soil and the soil-biochar mixtures, we determined the water retention curves using the pressure plate instrument. The curves were created considering the saturated and

residual water content as the maximum and minimum water content respectively. Figure 8 highlights the SWCCs of the different particle size fractions and application rates with CGW and BCM biochar. The boundary zone i.e. the upper part of the curve is considered the near saturation which is dominated by capillary effects near the air-water interface and occurs at low suction 0-50 kPa depending on the type of soil and pore structures (ASTM D6836). The curves show the stable saturation till there is a drop which is the air entry. For CGW biochar at the smallest particle size fraction (75–150  $\mu\text{m}$ ), all three application rates maintained high water content at low suction levels (1–50 kPa), with the 15% application rate retaining elevated water content across a broader suction range extending to approximately 100 kPa before declining sharply. 150–425  $\mu\text{m}$  showed similar water retention behavior until approximately 1000 kPa, where 15% app rate differed from 5% and 10% application rate. 425–850  $\mu\text{m}$  showed a gradual and more uniform drainage across the suction range compared to finer size fractions. For BCM, all size fractions showed a consistent retention across all application rate.

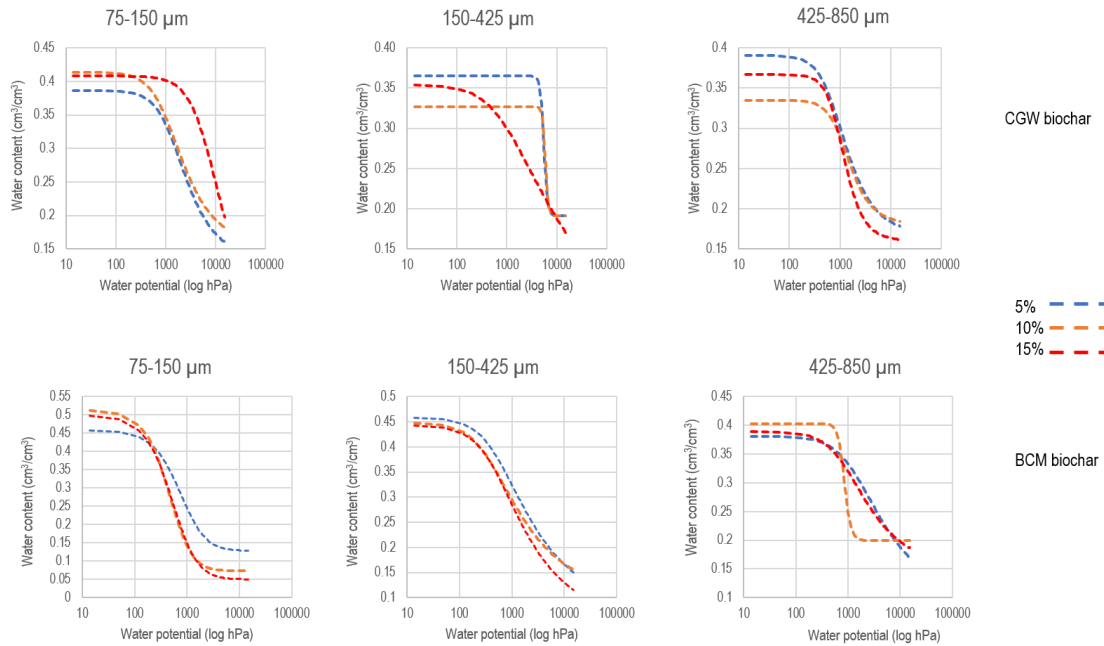


**Figure 9** Soil water characteristics curves for silt clay loam with CGW and BCM biochar (addition rate 5, 10 and 15%) across particle size fractions. The lines represent the fitted van Genuchten model

The shape of the curves is determined by  $n$ , which is a shape parameter in the van Genuchten model. High  $n$  values produce a very sharp and steep curve after air enters the soil. In CGW amended soils, 150–425  $\mu\text{m}$  at 5% and 10% application rate had  $n$  values of 12.24 and 15.13 respectively, which were different in shape compared to the other treatments. The corresponded  $n$  and air entry values from the van Genuchten model for each treatment are displayed in Table 6 .

**Table 6** van Genuchten  $\alpha$  and  $n$  values derived from different treatments using R software (\* = inconclusive)

	Treatment	$\alpha$ (1/kPa)	air entry value (kPa)	$n$	$R^2$
soil + cgw	75-150 (5%)	0.0077	130.6152	1.9110	0.9093
	75-150 (10%)	0.0098	101.9789	1.7994	0.9383
	75-150 (15%) *	0.0016	640.7521	1.7519	0.9289
	150-425 (5%) *	0.0018	546.1541	12.2428	0.9640
	150-425 (10%) *	0.0017	586.4263	15.1387	0.9941
	150-425 (15%)	0.0126	79.4995	1.2476	0.9127
	425-850 (5%)	0.0132	75.8374	2.0317	0.9457
	425-850 (10%)	0.0092	108.2712	2.4199	0.9547
	425-850 (15%)	0.0107	93.3582	2.7319	0.9761
soil + bcm	75-150 (5%)	0.0098	102.4252	1.5240	0.7670
	75-150 (10%)	0.0153	65.4103	1.6558	0.9055
	75-150 (15%)	0.0139	71.9267	1.5311	0.9998
	150-425 (5%)	0.0199	50.2104	1.4805	0.7677
	150-425 (10%)	0.0285	35.0526	1.5014	0.6594
	150-425 (15%)	0.0230	43.4821	1.5191	0.7657
	425-850 (5%)	0.0078	127.4211	1.5341	0.7207
	425-850 (10%)	0.0121	82.7778	7.3111	0.9817
	425-850 (15%)	0.0124	80.6869	1.6307	0.8515

The air entry values AEVs, which is considered the pressure at which drainage starts were observed to increase with biochar amendment. The highest AEVs were recorded for CGW amendment at 15% 75-150  $\mu\text{m}$ , 5% 150-425  $\mu\text{m}$  and 10% 150-425  $\mu\text{m}$ . Consistent with these results, these treatments also exhibited some of the least great  $\theta_{fc}$ . The regression model for the relationship between AEV and WHC generated an  $R^2 = 0.2$ , indicating a weak inverse linear trend that is, as AEV increases, WHC tends to decrease slightly, but the linear fit explains only 20% of the variation. This behavior suggests that the water drained from the pores between the soil and biochar and the water retained thereafter might be located between and within the biochar pores[21]. A similar statement was reported by Liu et al stating the water held at field capacity is dominated by intrapores

## 3.7 Statistical analysis report

### 3.7.1 Bulk density

ANOVA output demonstrate that bulk density was heavily influenced by the feedstock type, particle size and application rate, with strong interaction effects among these factors which were analyzed using the Tukey HSD test.

Individual factors indicate that feedstock ( $p < 0.001$ ) is highly significant. Ignoring all other factors, CGW and BCM biochars produce different bulk densities. Application rate produced a  $p < 0.001$  and had the largest F value, suggesting it is the strongest factor of bulk density change. Particle size also exhibited a very significant effect with a  $p < 0.001$  and F value of 10.074. Two-way interactions show that Feedstock-Application rate and Feedstock-Particle size were highly significant with each test yielding a p value  $< 0.001$ . However, the interaction between Application rate-Particle size shows a p value of 0.366, which suggests that the application rate and size do not interact consistently. This may also imply that the effects are additive not multiplicative. Many comparison interactions between feedstock were significant from the post hoc tests. Large significant differences were seen between different feedstocks, different application rate and different particle size but that trend wasn't consistent. However, particle size effect was significant with application rate but not as high compared to the application rate with feedstock. Overall the interaction between these three factors generated a p value of 0.026 which is statistically significant, suggesting that all three factors affect the soil's bulk density and that the way particle size influences the application rate is different for the type of biochar.

### 3.7.2 Water holding capacity (field capacity)

ANOVA analysis for field capacity showed feedstock was highly significant ( $F=106$ ,  $p < 0.001$ ), making it the dominant factor influencing water retention. Particle size followed steadily ( $F=19.38$ ,  $p < 0.001$ ) showing a notable effect. Contrary to these, application rate generated a  $p$  value of 0.07 with an  $F$  value of 2.719 indicating the lowest influence on field capacity water contents.

Interactions observed between Feedstock-Application rate ( $p = 0.03$ ) and Feedstock-Particle size ( $p < 0.001$ ) were significant. The strong significance of the Feedstock-Particle size indicates that the effect of particle size on water contents at field capacity is dependent on the feedstock type and that particle size has a greater influence than application within the same feedstock category.

The three factors interacting yielded a  $p$  value of 0.2, suggesting that they do not influence as a unit rather influence independently or through pairwise interactions.

This is supported with the Tukey HSD results. Comparisons between different feedstocks showed statistically significant differences, particularly within same particle size fractions. Significant differences were primarily associated with treatments involving feedstock and particle size confirmed significant differences ( $p < 0.0001$ ) but inconsistent significance seen between feedstock and application rate.

**Table 7** Three-way analysis of variance (ANOVA) for water holding capacity and bulk density as affected by feedstock type, application rate, and particle size, including all two-way and three-way interactions. Significance codes: '\*\*\*' p < 0.001, '\*' p < 0.05, '.' p < 0.1, 'ns' not significant.

Source of Variation	Bulk density			Water holding capacity		
	F Value	Pr(>F)	Sig.	F Value	Pr(>F)	Sig.
Feedstock	27.13	7.94e-06	***	106.084	8.35e-16	***
Application Rate	96.96	3.20e-15	***	2.719	0.0727	ns
Particle Size	10.07	0.003	***	19.383	1.84e-07	***
Feedstock × Application Rate	15.09	1.74e-05	***	3.678	0.0301	*
Feedstock × Particle Size	9.80	0.0004	***	13.778	8.58e-06	***
Application Rate × Particle Size	1.11	0.3656	ns	2.201	0.0773	ns
Feedstock × Application Rate × Particle Size	3.15	0.0255	*	1.588	0.1867	ns

## **4. DISCUSSION**

### **4.1 Effect of biochar particle size and application rate on water holding capacity**

Analyzing water contents across CGW and BCM biochar amendment, the effect varied considerably between them as well as across particle size ranges and application rates, which can be explained with the bulk density. As the bulk densities decreased, the water content at field capacity increase as a result of increased porosity. Due to its porous nature, biochar can adsorb and retain water. Particle size fractions had a causative effect in porosity of soil-biochar treatments. Across size fractions and applications, more of the particle sizes had more interpores. It's been reported by Liu et al [19] that intrapores increases water contents at field capacity, permanent wilting point, and a similar case is seen here when compared to the soil water characteristic curves.

Particle size governs the porosity pore size distributions and our research indicates that larger biochar sizes are more influential in changing overall porosity of the soil by a 27.66% increase. However, the highest increase in water holding was seen with smaller particle sizes. The analogy that a reduced bulk density leads to a decreased porosity and hence high-water holding capacity was not seen in silt clay loam. This could be related to the effective porosity of the soil-biochar mixtures which goes direct into the mesopore and micropore of the biochar. Our results suggest that water holding capacity and plant-available water are held within the mesopore network, more than in micropores, where water tightly bound

and largely unavailable for plant uptake and this is similar to reports from Edeh et al and Khaledi et al [18, 43] . Consequently, an adequate proportion of both mesopores and micropores is likely to enhance water dynamics, reducing the energy plants must expend to extract water from the soil matrix.

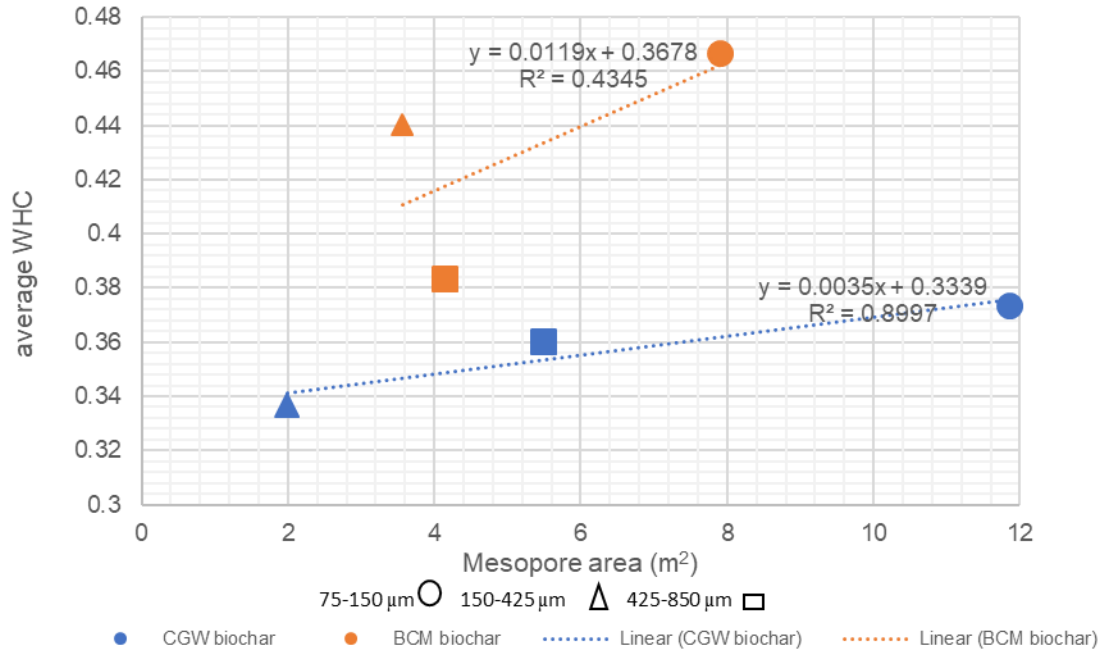


**Figure 10** Scatter plot diagram to compare average WHC across all particle size fractions to its mesopore area

Within CGW, the smallest particle size fraction (75–150 µm) exhibited the highest mesopore area (11.86) and correspondingly the highest WHC (0.37). Similar scenario occurred within BCM biochar and this reinforces that findings that mesopores play a key role in governing WHC particularly across particle size fractions.

Furthermore, SWCC depicts that all particle sizes contain a significant amount of macropores which are essential for water movement to the roots of plants. The ratio to of soil to biochars  $d_{50}$  were all less than 1. Introducing CGW and BCM biochars into soil

without size fractionation will result in an increase in macropores, since the biochars possess a coarser texture than the soil particles; yet, the internal porosity of the biochar will adequately hold water. Overtime, biochar breaks down into smaller fractions, enhancing soil water dynamics. Additionally, high application rates may not be beneficial in seeing an increment in soil water retention. Considering the cost of biochar per ton, our results show that a minimum dosage not surpassing 5% is sufficient to see an improvement in soil water retention and this increase the low-dose-high-efficiency benefits.

#### **4.2 Bulk density, surface area and porosity**

When biochar is added to soil, it contributes to the volume of the soil with an additional volume thereby increasing the total volume of the soil matrix. The bulk density of the soil will be lower than that of the original soil since the specific density of biochar is lower than that of soil. The trend seen here is that particle sizes recording the lowest specific density values lead to a lower bulk density in the soil. Increasing biochar application rates also reduced the bulk density across both materials; however, CGW biochar showed a stronger dependence on particle size, with larger particles significantly lowering the bulk density. In contrast, BCM biochar exhibited a more restrained response to particle size, with bulk density remaining relative the same with application rates increasing. This suggests that smaller particles fill in pore spaces in soil without strongly affecting the bulk density whereas coarser CGW particles enhance the macro porosity and reduce soil compaction. Blanco et al. [3] similarly reported that biochar application increased macroporosity, supporting patterns observed in our study. While application rate is a primary driver in bulk density reduction, the influence of particle size is strongly dependent on the type of

feedstock material biochar is made from which is similar to reports from Omondi et al and Joseph et al. [7, 41] .

Higher carbon contents directly correlate to a higher surface area and the addition of biochar in soil will indirectly increase the surface area and carbon content. Based on the biochar properties, we found that beef cattle manure generated the highest total organic carbon across both feedstocks which is contrary to 15.80% average reported by Bohran et al [37]. Even with the high TOC, the surface area was relatively lower compared to CGW. The unexpected high TOC observed in BCM biochar may be attributed to the diets and digestion complexes. Unlike pasture-based systems, feedlot manure represents are fed with typically high-energy grained based diet such as silage and steam-flaked corn and these the undigested feed residues excreted represent additional organic carbon. Lignocellulosic materials like cotton gin waste are mostly composed of organic structural compounds with relatively low ash content. The relationship between elemental composition and water retention did not follow conventional expectations in this study. While lower H/C ratios are typically associated with greater aromaticity and increased microporosity, which can enhance water retention, the results showed that BCM, despite exhibiting the highest H/C ratio, also recorded the highest water holding capacity. This indicates that a lower degree of aromatic condensation does not necessarily correspond to reduced water retention in this system. Similarly, the relatively narrow range of O/C ratios (0.15–0.21) suggests that surface oxygen functionality and by extension, hydrophilicity was comparable across treatments and therefore not the dominant controlling factor. Instead, these findings point to the importance of pore structure, particularly the development and distribution of mesopores, in governing water retention at water holding capacity. Biochars with less

condensed structures may promote greater pore volume and improved pore connectivity, enhancing their ability to store water after gravitational drainage.

Additionally, BCM having high TOC but lower surface area and an overall better mesopore area indicates that its pore network is dominated more by a good amount of mesopores than micropores which are essential for water retention. CGW, on the other hand, exhibited higher surface area and mesopore area in 75-150  $\mu\text{m}$  followed by 425-150  $\mu\text{m}$ , which explains the increased WHC. A higher surface area indicated more of biochar's external/macropore structure rather than the internal water holding pores.

#### **4.3 Effects of feedstock and application rate on hydraulic conductivity and infiltration**

Saturated hydraulic conductivity,  $K_{sat}$  is largely controlled by interpores (pores between soil and biochar particles) and macropores which facilitate rapid water movement. Biochars were sieved to coarser particle size fractions which contributes to lower bulk density and high macroposity between soil and biochar particles. Our results suggest that there are varying amounts of macropores especially with cotton gin waste biochar at each application rate. Comparing  $K_{sat}$  results with water retention, it supports the findings that macropores are more in CGW than BCM. Fine textured soils have compacted soil grains enabling them to hold more water and restrict water moving down the matrix. Although hydraulic conductivity has been reported increase or decrease or have no significant effect at all with biochar amendment in fine textured soils[17, 44], applying at high rates may increase saturated conductivity and over time, the breakdown of biochar will lead to tightly bounded water hold, leading to a decrease in  $K_{sat}$ . Additionally, despite thorough mixing, spatial variability in particle size distribution may persist, influencing pore structure and flow pathways. Infiltration rate describes how fast water enters the soil and it is controlled

by the pores within the soil matrix, and biochar has been reported to have little to no effect or a negative effect on fine clay loam soils' infiltration rate. Sun et al found that biochar application in silty loam soil was rate dependent. Lower biochar application rates increased infiltration rate while higher rates (5% and 10%) decreased infiltration[45] while higher application rates increased  $K_{sat}$ . Rebecca et al reported an increase  $K_{sat}$  in clay rich soil when biochar was added at a 10% rate [16]. The variations observed are likely due to the specific properties of the biochar used, structural change in disturbed soil and the conditions of the experiment. CGW application led to a noticeable enhancement at the infiltration rate and while BCM treatments demonstrated a low but more stable and consistent hydraulic behavior over time, which may be advantageous in field capacity if sustained infiltration capacity is desired. These findings suggest that designing biochar with appropriate pore characteristics can optimize pore size distribution within the soil matrix and enhance saturated hydraulic conductivity and infiltration and that the most influential factor is the feedstock type and the pyrolysis conditions. Juxtaposing saturated hydraulic conductivity to infiltration, a highly improved  $K_{sat}$  results to high infiltration rate at the start while a moderate improvement results in a low infiltration over time. These contrasting behaviors highlight that a higher  $K_{sat}$  does not necessarily translate to superior long-term infiltration performance, and that the pore structure conferred by feedstock characteristics ultimately governs the stability and sustainability of water movement in biochar-amended fine-textured soils.

#### **4.4 Soil water characteristics curve of soils with biochar addends**

Biochar effectiveness in increasing soil water retention varied in relation to its application rate and particle size fractions. Our findings suggest that all size fractions within 75-850

$\mu\text{m}$  are effective increasing soil water retention but dependent on the type of biochar. Comparing our air entry values to results to field capacity, lower air entry values retained greater water content, suggesting that biochar application resulted in the creation of large macropores. Air enters the soil at relatively low suctions which indicates that larger more connected pores are dominated in that region and a lower saturation levels means soil retains a significant amount of water at field capacity. Additionally, fine textured soils contain small pores that makes it hold water more than coarse grained, and the interaction here suggests the air entry value has an inverse relationship with water holding capacity. Moreover, this facilitates the drainage of materials like water and air into the underlying soil, making them easily accessible to plants. If the right biochar characteristics are improved specifically for certain soil-water property, the amount to add into the soil will be more prominent.

#### **4.5 Biochar influence on WHC or PAW in freshly made biochar mixtures versus field conditions.**

It is important to note that these results were obtained by mixing oven dried soil with biochar on a laboratory scale and we predict that translation into field capacity will reveal less than 50% of what our data suggests, given the size of field application and the natural state of the soil. We could have imitated field analysis in the lab but we needed a more controlled settings to design our biochar before moving to the field.

While ample research demonstrates biochar's ability to increase soil water holding capacity (WHC) and plant available water (PAW), a critical disconnect exists between controlled laboratory studies and long-term field performance. The physical and chemical mechanisms governing water retention evolve significantly as biochar transitions from a

freshly mixed amendment to an aged component of the soil matrix. Over longer field studies' timescales soil water retention properties due to biochar application are likely to be altered due to wetting/drying and freezing/thawing conditions, and soil structure evolution.

A study by R. Esmailnezhad et al reported no significant increase in the water holding capacity of biochar amended soils compared to undisturbed clay loam over a year[46]. Hardie et al found an increase in WHC but not in PAWC thirty months after field application of acacia green waste biochar[47]. Biochar undergoes processes that changes its composition and characteristics over time. Acharya et al review reported that biochar over time become more hydrophilic due to prolonged[12] exposure to water and oxygen while the breakdown of particle creates finer particles that fill inter-pore spaces, improving bulk density and microporosity[48] .Consequently, it is crucial to study the effects of biochar particle sizes on soil hydraulic properties in the field over an extended period of time.

## 5. CONCLUSION

In our study we assessed the role of biochar particle size, application rate and feedstock in soil water retention and movement in a laboratory setting. A combination of biochar particle size fractions within the micrometer range modifies water holding capacity with the feedstock material playing a crucial role in determining the biochar effects. Physical characteristics such as a reduced bulk density and an increased porosity are great contributors to soil water retention and transport in biochar-amended soils. Cotton gin waste biochar demonstrated more structurally dependent improvement, whereas beef cattle manure biochar demonstrated more stable and consistent improvements in all soil water measurements. Our results show biochar introduction into the soil contributes more to the pore size distribution of the fine textured soil and that water holding capacity is driven by the mesopores especially with the smaller particle sizes whereas macropores influence drainage which in turn improves hydraulic conductivity. The potential to detect a change is also dependent on the type of soil and how it interacts with the biochar present. Particle size fractions within this range (75-850  $\mu\text{m}$ ) also increased pore space distribution (interpores and intrapores) in silt clay loam and the ability to hold more water was more on the pores within the biochar (intrapores). Manure biochars are more labile whereas plant based biochars are more recalcitrant according to our elemental ratios. In water holding capacity, beef cattle manure's aliphatic structures promote pore accumulation by influencing particle aggregation and internal pore structure, which may support greater moisture retention in amended soil. We can say that BCM biochar can be effective in

increasing soil water capacity in a short term, while CGW biochar may play a significant role in holding water in a long term, stable water. Biochar had a noticeable impact on soil water characteristics, which does not follow a simple monotonous increasing or decreasing pattern with the increase of biochar. Most importantly, application rates beyond 5% did not yield proportional increase in soil water retention suggesting a minimal dose of biochar in fine textured are both economically and agronomically preferable.

Adding biochar to soil generally had a varied effect in silt clay loam's saturated conductivity and infiltration rate and the extent varied with different application rate and particularly biochar feedstock. The effect was due to the shift in pore distribution of biochar amended soils with cotton gin waste biochar promoting more macropores than beef cattle manure biochar. Fine textured soils naturally have tightly packed pores and slow water movement and when biochar is introduced, it drains water freely to reduce water logging risk and more water moves into the plant available rather being held. Our laboratory results should be considered as short term as changes in soil structure and hydrology changes overtime. Mechanisms such as microbial activities have been shown to increase soil aggregation and macroporosity, thereby altering saturated hydraulic conductivity and infiltration.

Overall, this study showed that it is possible to achieve significant changes in soil water retention in fine textured soil even if they already retain and move water better than coarse textured soils and with relatively low application rates. In particular PAW and WHC was found to increase most effectively with feedstock type that produce different physical and chemical properties based on the particle size fractions that contribute to pore structure in fine textured soil. This highlights that WHC and PAW are governed by the interactions

between feedstock type and particle size. Our results also indicate that the effects of biochar amendments on water retention and movement will depend on the pore structure which is in turn dependent on the biochar feedstock properties and particle size distribution. This amplifies the importance of tailoring biochar properties to suit specific hydraulic improvement targets, in order to maximize the effectiveness of biochar as a soil-water management tool.

## 6. REFERENCES

- [1] N. Howell, S. Bhattacharia, S. Aria, O. Garcia, C. Bednarz, and B. Guerrero, "Utilization of cotton gin waste biochars for agronomic benefits in soils," *Biomass Convers. Biorefinery*, vol. 15, no. 19, pp. 26449-26468, 2024, doi: 10.1007/s13399-024-05545-x.
- [2] R. Cen, W. Feng, F. Yang, W. Wu, H. Liao, and Z. Qu, "Effect mechanism of biochar application on soil structure and organic matter in semi-arid areas," *J Environ Manage*, vol. 286, p. 112198, May 15 2021, doi: 10.1016/j.jenvman.2021.112198.
- [3] H. Blanco-Canqui, "Biochar and Soil Physical Properties," *Soil Science Society of America Journal*, Review vol. 81, no. 4, pp. 687-711, Jul-Aug 2017, doi: 10.2136/sssaj2017.01.0017.
- [4] S. Mukhtar, "Manure-production-and-characteristics-its-importance-to-texas-animal-feeding-operations," *Texas A&M Agrilife Extension*.
- [5] USDA, "Cotton Ginnings 2024 Summary," National Agriculture Statistics Service, 2159-7804, 2025. [Online]. Available: <https://esmis.nal.usda.gov/sites/default/release-files/6108vb275/8s45s745q/n8711p389/ctgnan25.pdf>
- [6] S. A. Bhat *et al.*, "Application of Biochar for Improving Physical, Chemical, and Hydrological Soil Properties: A Systematic Review," *Sustainability*, vol. 14, no. 17, Sep 2022, Art no. 11104, doi: 10.3390/su141711104.
- [7] S. Joseph *et al.*, "How biochar works, and when it doesn't: A review of mechanisms controlling soil and plant responses to biochar," *Global Change Biology Bioenergy*, vol. 13, no. 11, pp. 1731-1764, Nov 2021, doi: 10.1111/gcbb.12885.
- [8] A. F. Zhang *et al.*, "Contrasting effects of straw and straw-derived biochar application on net global warming potential in the Loess Plateau of China," *Field Crops Research*, vol. 205, pp. 45-54, Apr 2017, doi: 10.1016/j.fcr.2017.02.006.
- [9] I. G. Edeh, O. Masek, and W. Buss, "A meta-analysis on biochar's effects on soil water properties - New insights and future research challenges," *Sci Total Environ*, vol. 714, p. 136857, Apr 20 2020, doi: 10.1016/j.scitotenv.2020.136857.
- [10] S. Adhikari, W. Timms, and M. A. P. Mahmud, "Optimising water holding capacity and hydrophobicity of biochar for soil amendment-A review," *Sci. Total Environ.*, vol. 851, Dec 2022, Art no. 158043, doi: 10.1016/j.scitotenv.2022.158043.
- [11] F. N. D. Mukome, X. Zhang, L. C. R. Silva, J. Six, and S. J. Parikh, "Use of Chemical and Physical Characteristics To Investigate Trends in Biochar

- Feedstocks," *Journal of Agricultural and Food Chemistry*, vol. 61, no. 9, pp. 2196-2204, 2013, doi: 10.1021/jf3049142.
- [12] B. S. Acharya *et al.*, "Biochar impacts on soil water dynamics: knowns, unknowns, and research directions," *Biochar*, vol. 6, no. 1, 2024, doi: 10.1007/s42773-024-00323-4.
- [13] Z. Q. Guo *et al.*, "Soil texture is an important factor determining how microplastics affect soil hydraulic characteristics," *Environment International*, vol. 165, Jul 2022, Art no. 107293, doi: 10.1016/j.envint.2022.107293.
- [14] S. K. Das, G. K. Ghosh, and R. Avasthe, "Valorizing biomass to engineered biochar and its impact on soil, plant, water, and microbial dynamics: a review," *Biomass Convers. Biorefinery*, vol. 12, no. 9, pp. 4183-4199, 2020, doi: 10.1007/s13399-020-00836-5.
- [15] C. J. Atkinson, J. D. Fitzgerald, and N. A. Hipps, "Potential mechanisms for achieving agricultural benefits from biochar application to temperate soils: a review," (in English), *Plant and Soil*, Review vol. 337, no. 1-2, pp. 1-18, Dec 2010, doi: 10.1007/s11104-010-0464-5.
- [16] R. T. Barnes, M. E. Gallagher, C. A. Masiello, Z. Liu, and B. Dugan, "Biochar-induced changes in soil hydraulic conductivity and dissolved nutrient fluxes constrained by laboratory experiments," *PLoS One*, vol. 9, no. 9, p. e108340, 2014, doi: 10.1371/journal.pone.0108340.
- [17] Z. Liu, B. Dugan, C. A. Masiello, R. T. Barnes, M. E. Gallagher, and H. Gonnermann, "Impacts of biochar concentration and particle size on hydraulic conductivity and DOC leaching of biochar–sand mixtures," *Journal of Hydrology*, vol. 533, pp. 461-472, 2016, doi: 10.1016/j.jhydrol.2015.12.007.
- [18] I. G. Edeh and O. Masek, "The role of biochar particle size and hydrophobicity in improving soil hydraulic properties," *European Journal of Soil Science*, vol. 73, no. 1, Jan 2022, doi: 10.1111/ejss.13138.
- [19] Z. Liu, B. Dugan, C. A. Masiello, and H. M. Gonnermann, "Biochar particle size, shape, and porosity act together to influence soil water properties," *PLoS One*, vol. 12, no. 6, p. e0179079, 2017, doi: 10.1371/journal.pone.0179079.
- [20] F. G. A. Verheijen, A. Zhuravel, F. C. Silva, A. Amaro, M. Ben-Hur, and J. J. Keizer, "The influence of biochar particle size and concentration on bulk density and maximum water holding capacity of sandy vs sandy loam soil in a column experiment," *Geoderma*, vol. 347, pp. 194-202, Aug 2019, doi: 10.1016/j.geoderma.2019.03.044.
- [21] Z. L. Liu, B. Dugan, C. A. Masiello, and H. M. Gonnermann, "Biochar particle size, shape, and porosity act together to influence soil water properties," *Plos One*, vol. 12, no. 6, Jun 2017, Art no. e0179079, doi: 10.1371/journal.pone.0179079.
- [22] A. E. Ajayi and R. Horn, "Modification of chemical and hydrophysical properties of two texturally differentiated soils due to varying magnitudes of added biochar," *Soil and Tillage Research*, vol. 164, pp. 34-44, 2016, doi: 10.1016/j.still.2016.01.011.

- [23] A. Igalavithana *et al.*, "Effect of Corn Residue Biochar on the Hydraulic Properties of Sandy Loam Soil," *Sustainability*, vol. 9, no. 2, 2017, doi: 10.3390/su9020266.
- [24] J. H. Chen *et al.*, "Response of microbial community structure and function to short-term biochar amendment in an intensively managed bamboo (*Phyllostachys praecox*) plantation soil: Effect of particle size and addition rate," (in English), *Sci. Total Environ.*, vol. 574, pp. 24-33, Jan 1 2017, doi: 10.1016/j.scitotenv.2016.08.190.
- [25] K. Rasa, J. Heikkinen, M. Hannula, K. Arstila, S. Kulju, and J. Hyväluoma, "How and why does willow biochar increase a clay soil water retention capacity?," *Biomass and Bioenergy*, vol. 119, pp. 346-353, 2018, doi: 10.1016/j.biombioe.2018.10.004.
- [26] J. Zhang, J. E. Amonette, and M. Flury, "Effect of biochar and biochar particle size on plant-available water of sand, silt loam, and clay soil," *Soil Tillage Res.*, vol. 212, Aug 2021, Art no. 104992, doi: 10.1016/j.still.2021.104992.
- [27] C. Pituello *et al.*, "Characterization of chemical–physical, structural and morphological properties of biochars from biowastes produced at different temperatures," *Journal of Soils and Sediments*, vol. 15, no. 4, pp. 792-804, 2014, doi: 10.1007/s11368-014-0964-7.
- [28] H. Wang, A. Garg, S. Huang, and G. Mei, "Mechanism of compacted biochar-amended expansive clay subjected to drying–wetting cycles: simultaneous investigation of hydraulic and mechanical properties," *Acta Geophysica*, vol. 68, no. 3, pp. 737-749, 2020, doi: 10.1007/s11600-020-00423-2.
- [29] X. Chen *et al.*, "Effect of Biochar on Soil-Water Characteristics of Soils: A Pore-Scale Study," *Water*, vol. 15, no. 10, 2023, doi: 10.3390/w15101909.
- [30] Q. Liu, N. Yasufuku, K. Omine, and H. Hazarika, "Automatic soil water retention test system with volume change measurement for sandy and silty soils," *Soils and Foundations*, vol. 52, no. 2, pp. 368-380, 2012, doi: 10.1016/j.sandf.2012.02.012.
- [31] F. Zhang, C. Zhao, S. D. N. Lourenço, S. Dong, and Y. Jiang, "Factors affecting the soil–water retention curve of Chinese loess," *Bulletin of Engineering Geology and the Environment*, vol. 80, no. 1, pp. 717-729, 2020, doi: 10.1007/s10064-020-01959-9.
- [32] C. Yang, J. Wu, P. Li, Y. Wang, and N. Yang, "Evaluation of Soil-Water Characteristic Curves for Different Textural Soils Using Fractal Analysis," *Water*, vol. 15, no. 4, 2023, doi: 10.3390/w15040772.
- [33] C. E. Brewer *et al.*, "New approaches to measuring biochar density and porosity," *Biomass and Bioenergy*, vol. 66, pp. 176-185, 2014, doi: 10.1016/j.biombioe.2014.03.059.
- [34] W.-T. Tsai, C.-H. Hsu, and Y.-Q. Lin, "Highly Porous and Nutrients-Rich Biochar Derived from Dairy Cattle Manure and Its Potential for Removal of Cationic Compound from Water," *Agriculture*, vol. 9, no. 6, 2019, doi: 10.3390/agriculture9060114.

- [35] W. J. Rawls, D. L. Brakensiek, and K. E. Saxton, "Estimation of Soil Water Properties," *Transactions of the ASAE*, vol. 25, no. 5, pp. 1316-1320, 1982, doi: <https://doi.org/10.13031/2013.33720>.
- [36] *Electrical Conductivity (EC) - Soil Health Guide*, N. R. C. Service, 1988.
- [37] M. S. Borhan, S. Rahman, and N. C. Sarker, "Characterizing Corn and Cattle Manure Derived Biochars Relevant to Their Use as Soil Additives," *Transactions of the ASABE*, vol. 61, no. 4, pp. 1335-1349, 2018, doi: <https://doi.org/10.13031/trans.12753>.
- [38] Y. F. Zhang, J. M. Wang, and Y. Feng, "The effects of biochar addition on soil physicochemical properties: A review," (in English), *Catena*, Review vol. 202, p. 19, Jul 2021, Art no. 105284, doi: 10.1016/j.catena.2021.105284.
- [39] N. Howell, A. Pimentel, and S. Bhattacharia, "Material properties and environmental potential of developing world-derived biochar made from common crop residues," *Environmental Challenges*, vol. 4, 2021, doi: 10.1016/j.envc.2021.100137.
- [40] F. U. Haider *et al.*, "An overview on biochar production, its implications, and mechanisms of biochar-induced amelioration of soil and plant characteristics," *Pedosphere*, vol. 32, no. 1, pp. 107-130, Feb 2022, doi: 10.1016/s1002-0160(20)60094-7.
- [41] M. O. Omondi, X. Xia, A. Nahayo, X. Y. Liu, P. K. Korai, and G. X. Pan, "Quantification of biochar effects on soil hydrological properties using meta-analysis of literature data," *Geoderma*, vol. 274, pp. 28-34, Jul 2016, doi: 10.1016/j.geoderma.2016.03.029.
- [42] M. A. D. L. b. Walter J. Rawls, Norman Miller, "Green-ampt Infiltration Parameters from Soils Data," *Journal of Hydraulic Engineering*, vol. 109, no. 1, 1983, doi: 10.1061.
- [43] S. Khaledi, M. Delbari, H. Galavi, H. Bagheri, and M. M. Chari, "Effects of biochar particle size, biochar application rate, and moisture content on thermal properties of an unsaturated sandy loam soil," *Soil and Tillage Research*, vol. 226, 2023, doi: 10.1016/j.still.2022.105579.
- [44] J. T. F. Wong, Z. Chen, A. Y. Y. Wong, C. W. W. Ng, and M. H. Wong, "Effects of biochar on hydraulic conductivity of compacted kaolin clay," *Environ Pollut*, vol. 234, pp. 468-472, Mar 2018, doi: 10.1016/j.envpol.2017.11.079.
- [45] W.-J. Sun, M.-Y. Li, W.-J. Zhang, and Y.-Z. Tan, "Saturated permeability behavior of biochar-amended clay," *Journal of Soils and Sediments*, vol. 20, no. 11, pp. 3875-3883, 2020, doi: 10.1007/s11368-020-02720-1.
- [46] R. Esmaeilnezhad, K. Zeinalzadeh, S. Besharat, and H. Kheirfam, "Field study on the hydraulic behavior of heavy soil: Effects of biochar application rates," *Sci Total Environ*, vol. 1004, p. 180752, Nov 15 2025, doi: 10.1016/j.scitotenv.2025.180752.

- [47] M. Hardie, B. Clothier, S. Bound, G. Oliver, and D. Close, "Does biochar influence soil physical properties and soil water availability?," *Plant and Soil*, vol. 376, no. 1-2, pp. 347-361, Mar 2014, doi: 10.1007/s11104-013-1980-x.
- [48] C. J. Atkinson, "How good is the evidence that soil-applied biochar improves water-holding capacity?," (in English), *Soil Use Manage.*, vol. 34, no. 2, pp. 177-186, Jun 2018, doi: 10.1111/sum.12413.